The turbulence scales of a wind turbine wake: A revisit of extended k-epsilon models

van der Laan, M P; Andersen, S J

Published in:
Journal of Physics: Conference Series

Link to article, DOI:
10.1088/1742-6596/1037/7/072001

Publication date:
2018

Document Version
Publisher's PDF, also known as Version of record

The turbulence scales of a wind turbine wake: A revisit of extended k-epsilon models

IOP Conf. Series: Journal of Physics: Conf. Series **1037** (2018) 072001 doi:10.1088/1742-6596/1037/7/072001

The turbulence scales of a wind turbine wake: A revisit of extended k-epsilon models

M P van der Laan[1] and S J Andersen[2]

[1]Technical University of Denmark, DTU Wind Energy, Risø Campus, DK-4000 Roskilde, Denmark
[2]Technical University of Denmark, DTU Wind Energy, Lyngby Campus, DK-2800 Kgs. Lyngby, Denmark

E-mail: plaa@dtu.dk

Abstract. The turbulence time and length scales of a single wind turbine wake subjected to atmospheric turbulence are calculated from two large eddy simulations that differ in ambient turbulence intensity. The smallest turbulence length scale in the wake is about half the rotor radius and it increases for higher ambient turbulence levels. The large eddy simulations are compared with Reynolds-averaged Navier-Stokes simulations employing the standard and three extended k-ε models: the k-ε-f_P model of van der Laan, the k-ε model of Shih and k-ε model of Durbin. It is shown that all three extended k-ε models can be written in a similar form. All Reynolds-averaged Navier-Stokes based turbulence models predict turbulence time scales that are comparable to the turbulence time scales of the large eddy simulations. The standard k-ε model underpredicts the velocity deficit because the turbulence length scale is overpredicted compared to the large eddy simulations. The performance of the k-ε model of Durbin shows to be very dependent on the ambient turbulence level and it is therefore less suited for wind turbine wake simulations. The k-ε model of Shih and the k-ε-f_P model of van der Laan are recommended to be used for wind turbine wake simulations because their results are similar and compare well with results of large eddy simulations for both a low and high ambient turbulence intensity due to a limitation of the turbulence length scale in the near wake.

1. Introduction

Wind turbine wakes can cause energy losses and increase wind turbine loads in wind farms. It is therefore important to model wake effects in order to design energy efficient wind farm layouts where wake induced loads are minimized and production maximized. There exists a variety of methods that model wake effects with different model fidelity, accuracy and computational costs. Engineering wake models [1] are fast but are often not very accurate. Large eddy simulation (LES) is a high fidelity Computational Fluid Dynamics (CFD) method where the most important scales of turbulence are resolved while the small scales of turbulence are modeled. LES has shown to model wakes accurately, but the computational cost is high due to its transient nature and the requirement of fine grid spacings. Reynolds-averaged Navier-Stokes (RANS) is a fast CFD method compared to LES because it is steady state and larger grid spacings can be used. RANS calculates the time averaged flow field directly and models all scales of turbulence. As a result, the turbulence model in RANS has a large influence on the results, which has been studied extensively [2]. A well known and widely used turbulence model is the k-ε model, which is known to underpredict the velocity deficit in the near wake due to an overprediction of the eddy

viscosity [2]. A number of RANS modelers [3, 4, 5, 6, 7] including ourselves, have developed new and applied existing extended k-ε models to overcome this issue. Most of these models limit the eddy viscosity in the wake by reducing the turbulence length and/or time scales. The extended k-ε models can show an improvement of the velocity deficit and turbulence intensity in the wake but not much is known about how well the limited turbulence length and time scales compare with those of LES. Moreover, it is not well known what the turbulence length and time scales of a wind turbine wake actually is. Several authors have fitted Kaimal spectra to temporal measurements [8] and LES data [9] of a single wind turbine wake and they have concluded that the fitted (Kaimal) length scale is in the order of the rotor radius. Troldborg [9] has also computed the integral turbulence length scale directly from LES data and found that the trends in the integral turbulence length scale as function of radial distance are comparable with the Kaimal length scale; however, the magnitude is different. In this work, we use LES data of two single wind turbine wake cases operating in atmospheric turbulence to investigate if the turbulence length and time scales from LES compare well with the turbulence length and time scales calculated by RANS using the standard and three extended k-ε models. A description of the extended k-ε models is presented in Section 2. A summary of the simulation methodology and description of the two single wake cases are given in Section 3. Two different methods of calculating the turbulence time and length scales directly from the LES data are presented in Section 4. Results of the two single wake cases are discussed in Section 5.

2. Description of standard and extended k-ε models

The standard and extended k-ε models are isotropic eddy viscosity models because they are based on a linear relation of the Reynolds-stress $\overline{u_i'u_j'}$ and the strain-rate tensor $2S_{ij} \equiv U_{i,j} + U_{j,i}$ following the Boussinesq approximation: $\overline{u_i'u_j'} = 2/3k\delta_{ij} - 2\nu_T S_{ij}$, where the eddy viscosity ν_T is a function of two scalar turbulence quantities; the turbulence kinetic energy k and the dissipation ε:

$$\nu_T = C_\mu \frac{k^2}{\varepsilon} f_P \tag{1}$$

Here C_μ is a model constant, which we set to 0.03, and in the extended k-ε models f_P is a scalar function that limits the eddy viscosity in regions where the magnitude of the velocity gradients is high. The product $C_\mu f_P$ can also be interpreted as a flow dependent C_μ [10, 11]. The f_P function is applied globally and one does not need to define regions where it should be applied (as required in the modified turbulence model of El Kasmi and Masson [3]). In addition, a transport equation for both k and ε is solved:

$$\frac{Dk}{Dt} = \nabla \cdot \left[\left(\nu + \frac{\nu_T}{\sigma_k} \right) \nabla k \right] + \mathcal{P} - \varepsilon, \qquad \frac{D\varepsilon}{Dt} = \nabla \cdot \left[\left(\nu + \frac{\nu_T}{\sigma_\epsilon} \right) \nabla \varepsilon \right] + \left(C_{\varepsilon,1}\mathcal{P} - C_{\varepsilon,2}\varepsilon \right) \frac{\varepsilon}{k} \tag{2}$$

where $\sigma_k = 1.0$, $\sigma_\epsilon = 1.3$, $C_{\varepsilon,1} = 1.21$ and $C_{\varepsilon,2} = 1.92$ are turbulence model constants, ν is the molecular kinematic viscosity (1.78×10^{-5}), and $\mathcal{P} = -\overline{u_i'u_j'}\partial U_i/\partial x_j$ is the turbulence production due to shear. The eddy viscosity can also be written as a function of two out of the three following turbulence scales: a turbulence length scale ℓ, a turbulence velocity scale u_* and a turbulence time scale τ:

$$\nu_T = u_*\ell = \frac{\ell^2}{\tau} = u_*^2\tau, \qquad u_* = C_\mu^{\frac{1}{4}} k^{\frac{1}{2}}, \qquad \ell = C_\mu^{\frac{3}{4}} \frac{k^{\frac{3}{2}}}{\varepsilon}, \qquad \tau = C_\mu^{\frac{1}{2}} \frac{k}{\varepsilon} \tag{3}$$

We choose to add the model constant C_μ to the definition of the turbulence scales because then the turbulence scales of the neutral atmospheric surface layer appear when inserting its solution

for k and ε ($k = u_*^2/\sqrt{C_\mu}$ and $\varepsilon = u_*^3/(\kappa z)$ in eq. (3): $\ell = \kappa z$ and $\tau = \kappa z/u_*$). In addition, one could choose to multiply f_P by one of the scales and interpret f_P as a limiter of one of the turbulence scales. It is possible to write the k-ε models of Shih et al. [10] (in a stationary frame of reference) and Durbin [12] in the form of the k-ε-f_P of van der Laan et al. [6], where the f_P functions are equal to:

$$\begin{array}{lll}
\text{standard:} & f_P = 1 & \\
\text{van der Laan:} & f_P = \dfrac{2f_0}{1+\sqrt{1+4f_0(f_0-1)\left(\frac{\sigma}{\tilde{\sigma}}\right)^2}} & f_0 = \dfrac{C_R}{C_R-1} \\
\text{Shih:} & f_P = \dfrac{f_0}{1+(f_0-1)\frac{\sigma}{\tilde{\sigma}}} & f_0 = \dfrac{1}{1-A_s/\tilde{\sigma}} \quad \dfrac{A_s}{\sqrt{6}} = \cos\left[\frac{1}{3}\arccos\left(\dfrac{\sqrt{6}S_{kl}S_{lm}S_{mk}}{(S_{kl}S_{lk})^{\frac{3}{2}}}\right)\right] \\
\text{Durbin:} & f_P = \min\left(f_0, \dfrac{1}{C_\mu \frac{k}{\varepsilon}\sqrt{6S_{kl}S_{lk}}}\right) & f_0 = 1
\end{array} \tag{4}$$

with $\sigma = k/\varepsilon\sqrt{(U_{i,j})^2}$ as the shear parameter, $\tilde{\sigma} = 1/\sqrt{C_\mu}$ as the constant shear parameter in the logarithmic surface layer and $C_R = 4.5$ as a model constant, which has been calibrated with LES for eight wake cases [6]. Figure 1 shows that the f_P functions have a comparable behavior with $\sigma/\tilde{\sigma}$, if we assume $S_{kl}S_{lm}S_{mk} = 0$ and $\sqrt{2S_{kl}S_{lk}} \approx \sigma$ (valid in the logarithmic surface layer). In the k-ε model of Durbin, f_P is also used to limit the turbulence time scale in

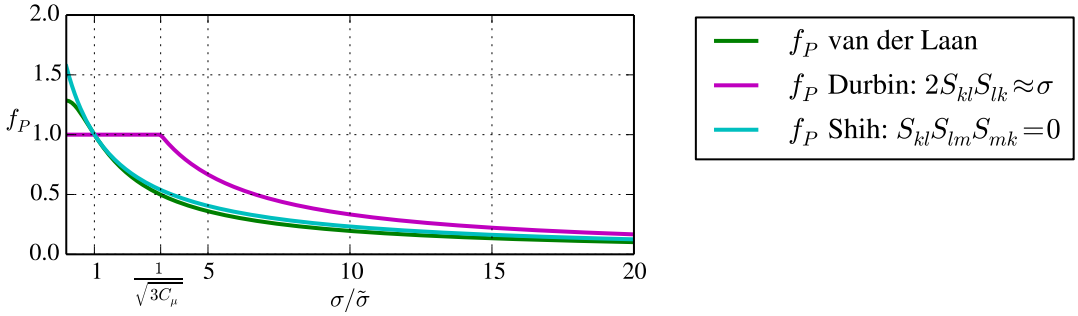

Figure 1. Comparison of f_P functions.

the transport equation of ε: $(C_{\varepsilon,1}\mathcal{P} - C_{\varepsilon,2}\varepsilon)\,\varepsilon/(kf_P)$, which we adapt in the present work. The f_P functions of the k-ε models of Durbin and Shih are derived in Appendix A.

Shih et al.[10] also proposed a modified transport equation of ε where the turbulent production due to shear $\mathcal{P} = \nu_T\mathcal{S}^2$ is replaced by $\mathcal{S}k$, where $\mathcal{S} \equiv \sqrt{2S_{kl}S_{lk}}$ and the constant $C_{\varepsilon,1}$ is a function of the normalized shear $\mathcal{S}k/\varepsilon$. We choose to use the standard transport equation of ε from eq. (2) such that a more fair comparison between turbulence models can be made.

3. Simulations and test cases

Two single wake cases are investigated which are based on a low and high ambient turbulence intensity case (Cases 5 and 6) from previous work [6], where also the simulation methodology is described in detail. A brief summary is presented here. The two cases represents the NREL-5MW reference wind turbine [13] modeled as an Actuator Disk (AD) [14, 15] that is operating at a constant thrust coefficient of 0.79 in a neutral atmospheric surface layer with a hub height velocity U_H of 8 m/s. The rotor diameter D and hub height z_H are 126 m and 90 m, respectively. The applied thrust and tangential force distributions are based on a detached eddy simulation of the NREL-5MW rotor, where the blade geometry is resolved in the grid. The ambient (total) turbulence intensity at hub height ($I_H = \sqrt{2/3k}/U_H$) is set to 4% and 12.8% for the low and

high turbulence case, respectively. The flow is solved by EllipSys3D [16, 17], which can both run LES and RANS simulations. In the LESs, the ambient turbulence is generated by the Mann model [18] and it is inserted at a cross plane, 1.5 D upstream of the AD. The inflow profiles represent a neutral logarithmic surface layer. In the RANS simulations, the roughness height is used to set the ambient turbulence intensity at hub height and the friction velocity is employed to set the freestream velocity at hub height. The same profiles are set in the LESs. The boundary conditions in the RANS simulations are in balance with the inflow profiles, where a rough wall boundary condition is used at the bottom of the domain [19]. In the LESs, a slip wall is used, which means that both the inflow profile and Mann turbulence develop downstream, although the changes are small enough to simulate a single wake in a near equilibrium turbulent shear flow. A fine uniformly spaced grid size of $D/60$ and $D/10$ is used around the AD in the LES and RANS simulation, respectively, which are based on previously performed grid studies [20, 15, 6].

4. Calculation of turbulence scales from LES

The calculation of the turbulence scales from an LES simulation is not trivial. In this article, two different methods are used following Troldborg [16] and are described in the preceding sections. In order to obtain statistically converged turbulence scales from the available 1 h LESs, we choose to sample the streamwise velocity at a polar grid and post-process ring-averaged (averaged over the azimuth) turbulence scales. The polar grid is oriented parallel to the AD with the origin at the AD center and has a spacing of $D/30$ and 3° in the radial and azimuthal directions, respectively. The data is extracted at three downstream distances $(x - x_{AD})/D = 2.5, 5, 7.5$ for every time step (0.24 s) for a duration of 1 h. Subsequently, the 1 h data is divided in six 10 minute bins and the turbulence scales are calculated for each bin. The final result of the turbulence scales represents the mean of the turbulence scales post-processed from the six 10 minute bins. In addition, an uncertainty of the mean of the six 10 minute bins is calculated as $\sigma/\sqrt{6}$, with σ as the standard deviation taken from the six bins.

For radii larger than the hub height, it is not possible to a ring-average over the whole azimuth due to the presence of the ground. This means that less data is included for large radii (for $r = 4R$, 73 of the 120 points are available).

One could argue that taking ring-averaged turbulence scales from a wind turbine operating in a shear is not ideal. However, since the wall boundary in the LESs is a slip wall and the inserted Mann turbulence is not connected to the wall boundary, the turbulence scales do not vary much with height, which allows the use of ring-averaging.

4.1. Method I: Integral turbulence time scale from autocorrelation

In this method, the integral turbulence time scale T is calculated by fitting an exponential function $\exp(-\tau/T)$ with a ring-averaged autocorrelation function. An example of an ring-averaged autocorrelation function and corresponding fit is shown in left plot of Figure 2 for the low ambient turbulence case at $(x - x_{AD})/D = 2.5$ and $r = 0.5R$. It is possible to obtain a turbulence length scale by multiplying the ring-averaged integral turbulence time scale by a velocity scale (ring-averaged streamwise velocity) if Taylor's frozen turbulence hypothesis applies.

4.2. Method II: Fit with Kaimal spectrum

The Kaimal spectrum from the IEC standard [21] is defined as (for the stream-wise direction):

$$S_k = 4\sigma_k^2 \frac{L_k/U_H}{(1 + 6fL_k/U_H)^{(5/3)}}, \tag{5}$$

where σ_k is the standard deviation, L_k is the Kaimal length scale, f is the frequency and U_H is the freestream velocity at hub height. The Kaimal spectrum is fitted with ring-averaged spectra,

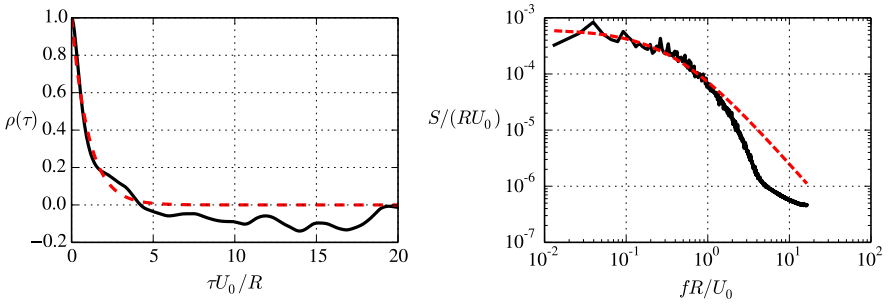

Figure 2. Left plot, Method I: Example of a fitted exponential function ($T = 8.3$ s, red) with a ring-averaged autocorrelation (black). Right plot, Method II: Example of fitted Kaimal spectrum ($\sigma_k = 0.15$ m/s, $L_k = 28$ m, red) with ring-averaged spectrum (black).

where both σ_k and L_k are used as variables to be fitted. An example of a fitted Kaimal spectrum for the low ambient turbulence case at $(x - x_{AD})/D = 2.5$ and $r = 0.5R$ is shown in the right plot of Figure 2. The fit is performed in the linear domain and therefore aimed at matching the low frequencies.

5. Results and Discussion

5.1. Turbulence scales from LES

The turbulence length scale calculated from the two LESs (as discussed in Section 4) are shown in Figure 3, for three downstream distances. The shaded area represents the uncertainty of the

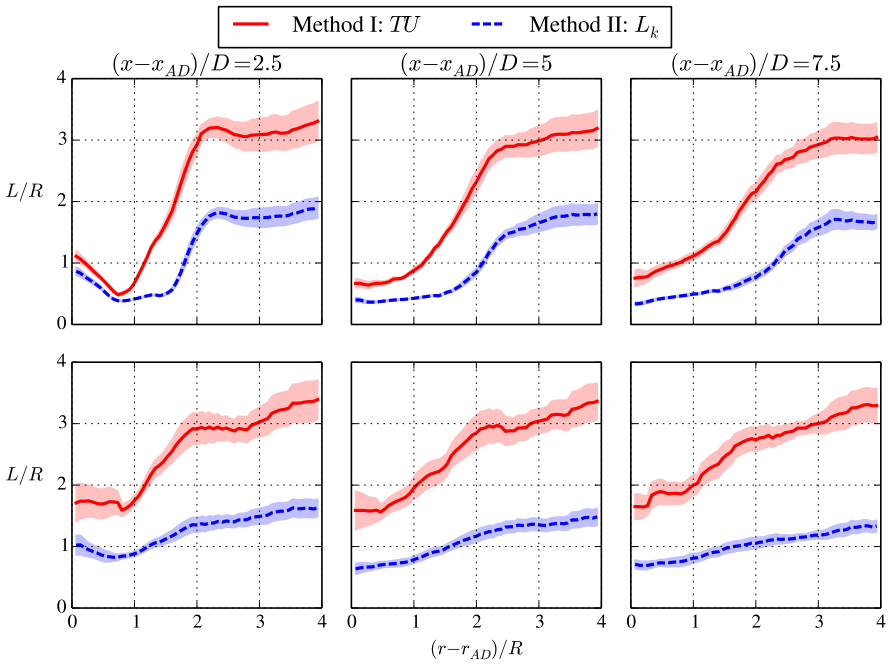

Figure 3. Turbulence length scale from LESs computed with two different methods for three downstream distances. Top row: low ambient turbulence case, bottom row: high ambient turbulence case. Shaded area represents the uncertainty of the mean of six 10 min averages.

mean, calculated from the six 10 minute bins. For both ambient turbulence cases, Method I predicts larger length scales (TU) than method II (L_k), which could be explained by the fact that L_k is only a model parameter and not a physical turbulence length scale as TU. In addition, Taylor's frozen turbulence hypothesis might not be valid for a wind turbine wake. It is clear from Figure 3 that the turbulence length scale is smaller inside the wake compared to the turbulence length scale in the freestream, where the smallest turbulence length scale is around half the rotor radius for the low ambient turbulence intensity case. For the high ambient turbulence case (bottom row plots of Figure 3), the turbulence length scale of the wake is larger and the difference between the methods is more pronounced compared to the low ambient turbulence case.

5.2. Comparison of turbulence models

The streamwise velocity at hub height normalized by the freestream is plotted in Figure 4, for the low (left column) and high (right column) ambient turbulence intensity cases, respectively. The freestream in the LESs is calculated by LESs without an AD to account for the small imbalance of the shear and the no slip wall. Results of all turbulence models are shown. The standard k-ε model underpredicts the velocity deficit compared to LES as expected, especially for the low ambient turbulence intensity case. Figure 4 shows that the k-ε-f_P model and the k-ε model of Shih predict similar velocity deficits that also compare well with LES for both ambient turbulence intensity cases. For the low ambient turbulence case (left column of Figure 4), the velocity deficit predicted by the k-ε model of Durbin is longer and has a more distinct pointed shape compared to LES, while for the high ambient turbulence case (right column of Figure 4), the velocity deficit predicted by the k-ε model of Durbin is similar to the standard k-ε model and it underpredicts the velocity deficit in the near wake compared to LES. This shows that the performance of the k-ε model of Durbin is very sensitive to the level of ambient turbulence.

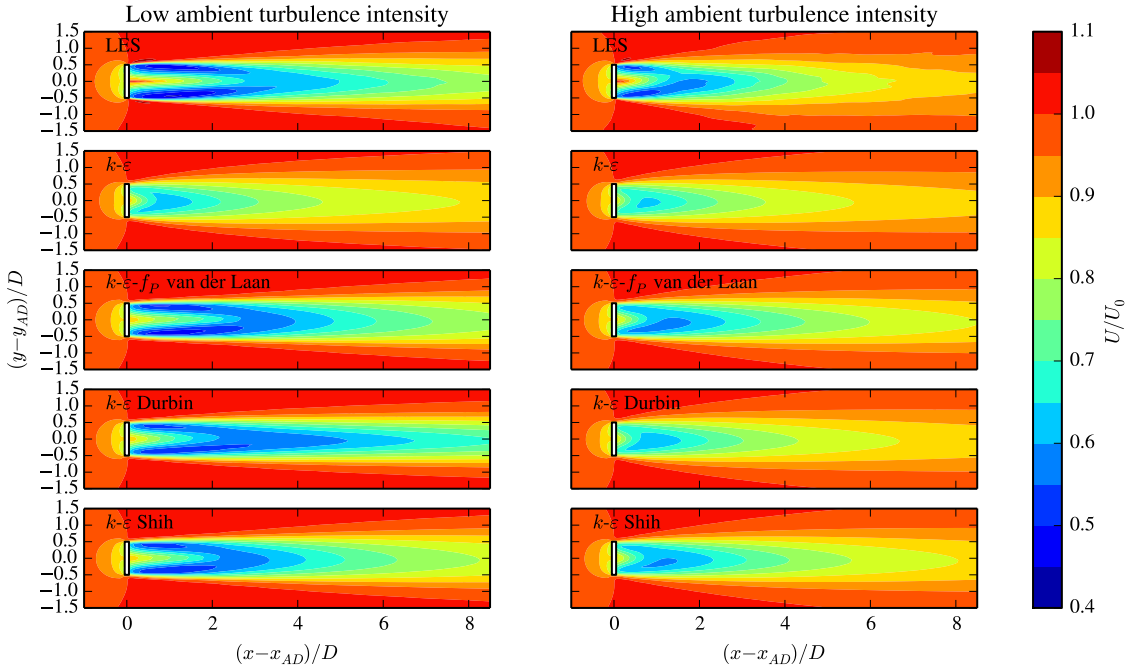

Figure 4. Comparison of all turbulence models for contours of streamwise velocity.

In Figure 5, a comparison between the standard and the extended k-ε models is made with

LES for the total turbulence intensity added by the wake (where $I = \sqrt{2/3k}/U_0$, top row), the turbulence time scale (middle row) and the turbulence length scale (bottom row) for the low ambient turbulence intensity case at three downstream distances. The added total turbulence intensity in the LES is calculated by subtracting the total turbulence intensity by a LES without an AD to account for the downstream decay of the Mann turbulence. All results in Figure 5 are taken from a spanwise line at hub height, except for the ring-averaged turbulence time and length scales from LES, as discussed in Section 4. Hence the turbulence time and length scales from LES are symmetric due to the ring-averaging procedure. In order to compare the turbulence scales from RANS with LES, the turbulence scales are normalized by the turbulence scales taken from a simulation without an AD. The LES turbulence time and length scales are calculated with Method I and Method II, respectively, to avoid the need of the Taylor's frozen turbulence hypothesis. In addition, the shaded area around the LES results represents the uncertainty of the mean of six 10 minute bins.

The added turbulence intensity in the near wake (top row, left plot of Figure 5) is better predicted by the extended k-ε models compared the standard k-ε model. Further downstream, the turbulence intensity from all RANS models is overpredicted compared to LES.

The wake recovery of the k-ε model of Durbin is slower compared to wake recovery calculated by the LES and the other two extended k-ε models, as shown previously in Figure 4. This is caused by the fact that the f_P function in the k-ε model of Durbin is not only used to limit the eddy viscosity but also employed to limit the turbulence time scale in the transport equation for ε. The effect of this extra limitation is also visible in the comparison of turbulence time and length scales in Figure 5 (middle and bottom rows), where k-ε model of Durbin has the lowest turbulence time and length scales in the far wake ($x - x_{AD} > 2.5D$).

Surprisingly, all models, including the standard k-ε model predict turbulence time scales in the wake that are comparable with the integral turbulence time scale calculated by LES. The bottom row of Figure 5 shows that the standard k-ε model calculates turbulence length scales that are much higher than the undisturbed turbulence length scale. This indicates that the standard k-ε model is underpredicting the velocity deficit because of an overprediction in the turbulence length scale.

The k-ε-f_P and the k-ε model of Shih limit the turbulence length scale in the near wake where the velocity gradients are the highest, while further downstream, the turbulence length scale recovers towards the standard k-ε model. In previous work [11], we have argued that k-ε-f_P acts as a turbulence length scale limiter and Figure 5 confirms this. The turbulence length scale of the k-ε model of Durbin hardly recovers over a downstream distance of 7.5D but compares best with the turbulence length scale of LES. Overall, the k-ε-f_P and the k-ε model of Shih show very similar results because their f_P functions are comparable, as shown in Figure 1.

Results for the high ambient turbulence intensity case are shown in Figure 6 and are presented in the same form as Figure 5. The differences between the turbulence models for the high ambient turbulence intensity case are much smaller compared to the low ambient turbulence intensity case, which has also been observed in previous work [6, 22]. Surprisingly, Figure 6 shows that the k-ε model of Durbin behaves almost the same as the standard k-ε model (see turbulence length scale in the near wake as shown in the bottom row left plot of Figure 6), while the low ambient turbulence intensity case (Figure 5) indicates that k-ε model of Durbin differs the most from the standard k-ε with respect to the other extended k-ε models. This shows that the performance of the k-ε model of Durbin is very sensitive to ambient turbulence intensity, which makes the model less suited for wind turbine wake simulations compared to the k-ε-f_P model and the k-ε model of Shih.

The comparison of the turbulence time scale (middle row of Figure 6) from LES with the RANS is challenging for high ambient turbulence intensity, since the integral turbulence time scale in the wake is not much smaller than the ambient integral turbulence time scale. The

turbulence length scale (bottom row of Figure 6) is more pronounced in the LES, and the k-ε-f_P model and the k-ε model of Shih show similar trends in the near wake but not in the far wake.

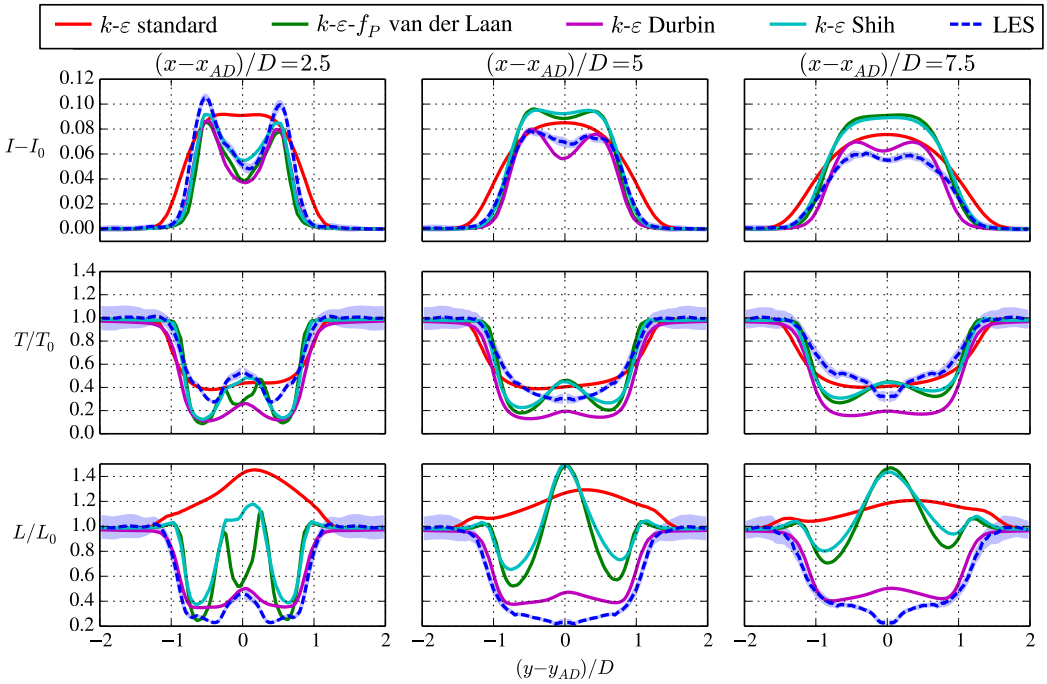

Figure 5. Comparison of turbulence models for the low ambient turbulence case. Shaded area represents the uncertainty of the mean of six 10 min averages for the post-processed LES results.

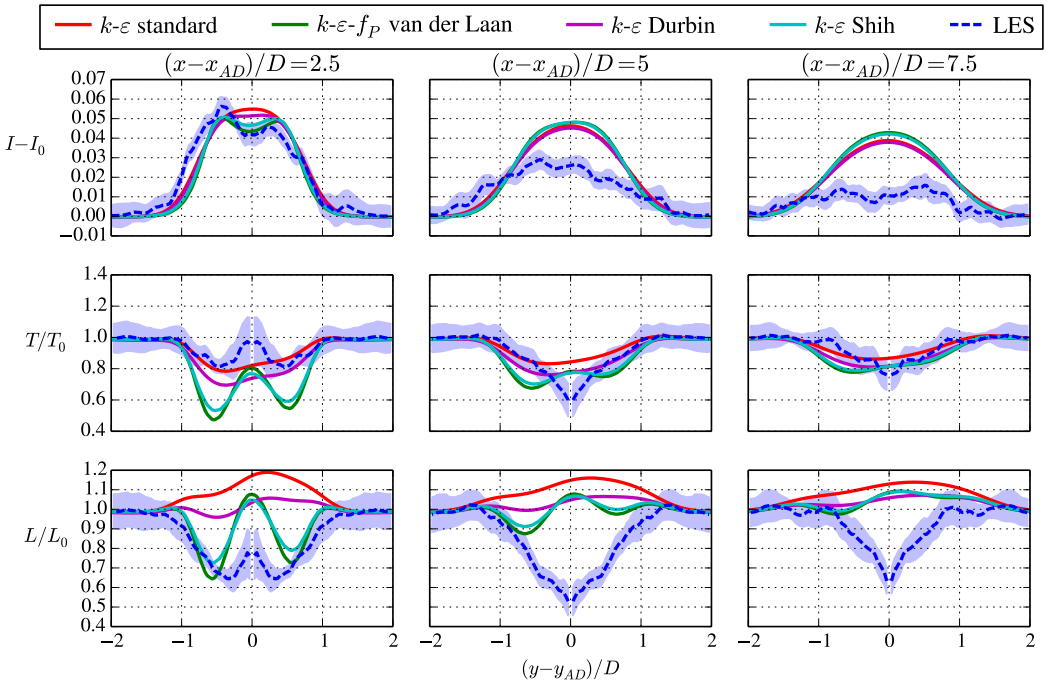

Figure 6. Comparison of turbulence models for the high ambient turbulence case. Shaded area represents the uncertainty of the mean of six 10 min averages for the post-processed LES results.

All RANS-based turbulence models require a similar amount of computational resources as reported in previous work [6].

6. Conclusions

The turbulence time and length scales of a single wind turbine wake operating in atmospheric turbulence are calculated from two LESs that differ in ambient turbulence intensity. Two methods are used to calculate the turbulence scales: a method based on fitting an exponential function with the autocorrelation to obtain a turbulence time scale and a method based on fitting a Kaimal spectrum to extract a turbulence length scale. The smallest turbulence length scale in the wake is found to be half the rotor radius and it increases with higher ambient turbulence levels. The calculated turbulence scales from LES are compared with RANS simulations employing the standard k-ε model and three extended k-ε models: the k-ε-f_P model of van der Laan, the k-ε model of Shih and k-ε model of Durbin, which can all be written in the form of the k-ε-f_P model. All RANS models, including the standard k-ε model, predict turbulence time scales that compare well with LES. The standard k-ε model underpredicts the velocity deficit because the turbulence length scale is overpredicted compared to LES. The k-ε-f_P model and k-ε model of Shih show very similar results that compare well with LES in terms of velocity deficit, turbulence intensity in the near wake, turbulence time scale and turbulence length scale in the near wake for both low and high ambient turbulence intensity because of a limitation of the turbulent length scale in the near wake. The turbulence length scale in the far wake is overpredicted by the k-ε-f_P model and k-ε model of Shih because both models recover towards the results of the standard k-ε model with downstream distance. For low ambient turbulence intensity, the k-ε model of Durbin has a too low wake recovery compared to LES because the f_P function is both used to limit the eddy viscosity and the source terms in the transport equation of ε which could be interpreted as double counting. For high ambient turbulence, the k-ε model of Durbin behaves very similar as the standard k-ε model. Since the performance of the k-ε model of Durbin shows to be very dependent on the ambient turbulence level, it is less suited to be used for wind turbine wake simulations where the ambient turbulence level is an important input parameter. We recommend to employ either the k-ε model of Shih or the k-ε-f_P model because they compare well with LES for both low and high ambient turbulence intensities.

Appendix A. Derivations of f_P functions

Appendix A.1. k-ε model of Durbin

The turbulence model of Durbin limits the turbulence time scale $\mathcal{T}$ as:

$$\mathcal{T} = \min\left(\frac{k}{\varepsilon}, \frac{1}{C_\mu\sqrt{6S_{kl}S_{lk}}}\right) \tag{A.1}$$

The limited turbulence time scale is used in the eddy viscosity:

$$\nu_T = C_\mu k\mathcal{T} \tag{A.2}$$

and in the transport equation for ε:

$$\frac{D\varepsilon}{Dt} = \nabla\cdot\left[\left(\nu + \frac{\nu_T}{\sigma_\epsilon}\right)\nabla\varepsilon\right] + \left(C_{\varepsilon,1}\mathcal{P} - C_{\varepsilon,2}\varepsilon\right)\frac{1}{\mathcal{T}} \tag{A.3}$$

The equivalent f_P function can be obtained by:

$$f_P \equiv \mathcal{T}\frac{\varepsilon}{k} \tag{A.4}$$

Appendix A.2. k-ε of model of Shih

The original model of Shih et al. [10] uses a variable C_μ (C_μ^*), which is defined as (in a stationary frame of reference):

$$C_\mu^* = \frac{1}{A_0 + A_s\sigma}, \qquad A_s = \sqrt{6}\cos\left[1/3\arccos\left(\sqrt{6}\frac{S_{kl}S_{lm}S_{mk}}{(S_{kl}S_{lk})^{(3/2)}}\right)\right] \tag{A.5}$$

with A_0 as a constant. The actual C_μ is only a function of A_0, since in the logarithmic surface layer we have $S_{kl}S_{lm}S_{mk} = 0$, which gives $A_s = 3/\sqrt{2}$ (and not $S_{kl}S_{lm}S_{mk} = S_{13}^3/2$ and $A_s = \sqrt{6}$ as reported in Cabezon et al.[4]), and $\tilde{\sigma} = 1/\sqrt{C_\mu}$. For a given C_μ, A_0 can then be expressed as:

$$C_\mu = \frac{1}{\tilde{\sigma}^2} = \frac{1}{A_0 + A_s\tilde{\sigma}} \quad \Rightarrow \quad A_0 = \tilde{\sigma}\left(\tilde{\sigma} - A_s\right) = \frac{1 - A_s\sqrt{C_\mu}}{C_\mu} = \frac{1 - \frac{3}{2}\sqrt{2C_\mu}}{C_\mu} \tag{A.6}$$

To obtain the equivalent f_P function, one can write:

$$f_P \equiv \frac{C_\mu^*}{C_\mu} = \frac{f_0}{1 + (f_0 - 1)\,\frac{\sigma}{\tilde{\sigma}}}, \quad f_0 = 1 + \tilde{\sigma}\frac{A_s}{A_0} \tag{A.7}$$

The constant A_0 can be eliminated using eq. (A.6):

$$f_0 = \frac{1}{1 - A_s/\tilde{\sigma}} \tag{A.8}$$

References

[1] Göçmen T, van der Laan M P, Réthoré P E, Peña Diaz A, Larsen G C and Ott S 2016 *Renewable and Sustainable Energy Reviews* **60** 752
[2] Réthoré P E 2009 *Wind Turbine Wake in Atmospheric Turbulence* Ph.D. thesis Risø
[3] El Kasmi A and Masson C 2008 *Journal of Wind Engineering and Industrial Aerodynamics* **96** 103
[4] Cabezón D, Migoya E and Crespo A 2011 *Wind Energy* **14** 909
[5] Prospathopoulos J M, Politis E S, Rados K G and Chaviaropoulos P K 2011 *Wind Energy* **14** 285
[6] van der Laan M P, Sørensen N N, Réthoré P E, Mann J, Kelly M C, Troldborg N, Schepers J G and Machefaux E 2015 *Wind Energy* **18** 889
[7] Hennen J and Kenjereš S 2017 *International Journal of Heat and Fluid Flow* **68** 319
[8] Larsen G C, Hansen K S, J M, Enevoldsen K and Bingöl F 2010 *Procedings from TORQUE 2010*
[9] Troldborg N 2009 *Actuator Line Modeling of Wind Turbine Wakes* Ph.D. thesis Technical Univeristy of Denmark, Department of Mechinical Engineering, Lyngby, Denmark
[10] Shih T H, Liou W W, Shabbir A, Yang Z and Zhu J 1994 A new *k-ε* eddy viscosity model for high Reynolds number turbulent flows-model development and validation Tech. rep. NASA
[11] van der Laan M P, Hansen K S, Sørensen N N and Réthoré P E 2015 *Journal of Physics: Conference Series* **524** 1
[12] Durbin P A 1996 *Int. J. Heat and Fluid Flow* **17** 89–90
[13] Jonkman J, Butterfield S, Musial W and Scott G 2009 Definition of a 5-MW Reference Wind Turbine for Offshore System Development Tech. rep. National Renewable Energy Laboratory
[14] Mikkelsen R 2003 *Actuator Disc Methods Applied to Wind Turbines* Ph.D. thesis DTU
[15] Réthoré P E, van der Laan M P, Troldborg N, Zahle F and Sørensen N N 2013 *Wind Energy* Pub. online
[16] Sørensen N N 1994 *General purpose flow solver applied to flow over hills* Ph.D. thesis DTU
[17] Michelsen J A 1992 Basis3d - a platform for development of multiblock PDE solvers. Tech. rep. DTU
[18] Mann J 1994 *Journal of Fluid Mechanics* **273** 141
[19] Sørensen N N, Bechmann A, Johansen J, Myllerup L, Botha P, Vinther S and Nielsen B S 2007 *Journal of Physics: Conference series* **75** 1
[20] Troldborg N, Sørensen J N and Mikkelsen R 2010 *Wind Energy* **13** 86–99
[21] *IEC 61400-1 Ed. 3 (2005): Wind turbines - Part 1: Design requirements. International Electrotechnical Commission.*
[22] van der Laan M P, Sørensen N N, Réthoré P E, Mann J, Kelly M C, Troldborg N, Hansen K S and Murcia J P 2015 *Wind Energy* **18** 2065